J. KSIAM Vol.13, No.2, 141–159, 2009

ADAPTIVE CVT-BASED REDUCED-ORDER MODELING OF BURGERS EQUATION

GUANG-RI PIAO[1], QIANG DU[2], AND HYUNG-CHUN LEE[3†]

[1]DEPARTMENT OF MATHEMATICS, YANBIAN UNIVERSITY, YANJI 133002, CHINA
E-mail address: piaogr@hanmail.net

[2]DEPARTMENT OF MATHEMATICS, PENNSYLVANIA STATE UNIV., UNIVERSITY PARK, PA 16802, USA
E-mail address: qdu@math.psu.edu

[3] DEPARTMENT OF MATHEMATICS, AJOU UNIVERSITY, SUWON, SOUTH KOREA 443-749
E-mail address: hclee@ajou.ac.kr

ABSTRACT. In this article, we consider a weighted CVT-based reduced-order modelling for Burgers equation. Brief review of the CVT (centroidal Voronoi tessellation) approaches to reduced-order bases are provided. In CVT-reduced order modelling, we start with a snapshot set just as is done in a POD (Proper Orthogonal Decomposition)-based setting. So far, the CVT was researched with uniform density ($\rho(\mathbf{y}) = 1$) to determine the basis elements for the approximating subspaces. Here, we shall investigate the technique of CVT with nonuniform density as a procedure to determine the basis elements for the approximating subspaces. Some numerical experiments including comparison of two CVT (CVT-uniform and CVT-nonuniform)-based algorithm with numerical results obtained from FEM(finite element method) and POD-based algorithm are reported.

1. INTRODUCTION

Research of reduced-order models to the computational simulation for (nonlinear) complex systems has recently received an increasing amount of attention. Since the standard discretization schemes (finite element, finite difference, finite volume, etc.) may require a great number of degrees of freedom for the accurate simulation of partial differential equations, applications of these approaches are expensive with respect to both storage and computing time. Roughly speaking, the reduced-order approach is based on projecting a complex dynamical system onto a simple manifold (possibly a linear subspace spanned by some basis elements) that contain

Received by the editors May 12 2009; Accepted May 30 2009.
2000 *Mathematics Subject Classification.* 49J20, 76D05, 49B22, 93B05.
Key words and phrases. reduced-order modelling, proper orthogonal decomposition, centroidal Voronoi tessellations, Burgers equation.
This work was supported by KRF-2005-070-C00017. Q. Du was partially supported by NSF DMS 0712744.
† Corresponding author.

characteristics of the expected solution. This is in contrast to the traditional numerical methods such as conventional finite element techniques where the elements of the subspaces are uncorrelated to the physical properties of the system that they approximate.

The ideas underlying the reduced-basis method appear to have their origins in the suggestions of Almroth [1] and Nagy [26], which were developed by Noor and colleagues [27]-[29] in the context of simulations for structures and later by Peterson [30] in high Reynolds numbers incompressible viscous flow simulations. In a nut-shell, the reduced-basis method employs parameter-dependent solutions of the system to be approximated. These solutions are used to construct basis elements in the hope that solutions at other parameter values can be represented in terms of perturbations of solutions given at carefully chosen parameter values (the Lagrange basis approach) or in terms of a "moving frame" (the Taylor approach). It is important to note that the parameter-dependent solutions used as basis functions can be obtained either from full-order model numerical simulations or experimental data.

The POD technique has been widely discussed in the literature of the past twenty years and replaced as a tool for model reduction (see [3, 19, 20] and the references cited therein). The centroidal Voronoi tessellation (CVT) as reduced order modelling technique is an active research field. Centroidal Voronoi tessellation-based reduced-order modelling of fluid flows was developed by [21, 22]. In CVT-reduced order modelling, we start with a snapshot set just as is done in a POD-based setting. However, instead of determining a POD basis from the snapshot set, we apply our CVT methodologies to determine the generators of a CVT of the snapshot set; these generators constitute the reduced-order basis. We then use the CVT-based basis in just the same way as one uses a POD-based basis to determine a very low-dimensional approximation to the solution of a complex system. CVT also possesses an optimality property, although it is different from that possessed by POD bases. In this article, we shall investigate the CVT method as a reduced order model for the unsteady Burgers equation with appropriate initial and boundary conditions. As a matter of fact, POD and CVT may be viewed as simply different procedures to determine the basis elements for the approximating subspaces. A more general framework, CVOD, that combines CVT with POD has also been proposed [9, 14].

So far, the CVT reduced-order modelling problems have been studied in uniform density ($\rho(\mathbf{y}) = 1$)(see [21]). We term this case "CVT-uniform". However, sometimes the generators obtained by CVT-uniform do not lead to satisfactory results in the reduced-order modelling problems (see [21, 22]). Therefore, to overcome this disadvantage, we extend the uniform density to more general nonuniform densities (variable densities). We term this case "CVT-nonuniform". From the reduced-order basis obtained by CVT-nonuniform, we may achieve better results in the reduced-order model problems. In this article, we shall investigate the technique of CVT-nonuniform method as a procedure to determine the basis elements for the approximating subspaces.

The plan for the rest of paper is as follows. In section 2, we give some definitions and property of CVT's, and two approaches for computing these tessellations. In addition, a CVT-nonuniform algorithm is introduced. Section 3 is devoted to applying CVT to solve the time-dependent Burgers equation. In section 4, some numerical experiments including comparisons of the CVT-uniform and CVT-nonuniform algorithms and POD-based algorithm are reported

based on numerical results from FEM simulations. Then we make concluding remarks in Section 5.

2. CENTROIDAL VORONOI TESSELLATION BASED MODEL REDUCTION

The concept of the *centroidal Voronoi Tessellations* (CVTs) has been studied in [13]. CVTs have been successfully used in several data compression settings, e.g., in image processing and the clustering of data. Reduced-order modelling of complex systems is another data compression setting, i.e., one replaces high-dimensional approximations with low-dimensional ones. CVTs can be used for this purpose as well.

We here consider the case where we are driven a discrete set of points $\mathcal{S} = \{\mathbf{y}_j\}_{j=1}^M$ consisting of M vector belonging to $\mathbb{R}^N$. The concept of centroidal Voronoi tessellations (CVTs) can be extended to more general sets, including regions in Euclidean space, and to more general metrics; for detailed discussions, see [13].

2.1. Definition of CVTs for discrete data sets.

The definition of CVT's for discrete data sets begins with a set $\mathcal{S} = \{\mathbf{y}_j\}_{j=1}^M$ consisting of M vectors belonging to $\mathbb{R}^N$. Of course, $\mathcal{S}$ can also be viewed as a set of M points in $\mathbb{R}^N$ or a possibly complex-valued $N \times M$ matrix. In the context of CVT, it will be useful to think of the columns $\{S_{\cdot,j}\}_{j=1}^M$ of $\mathcal{S}$ as the spatial coordinate vectors of a dynamical system at time t_j. Similarly, we consider the rows $\{S_{i,\cdot}\}_{i=1}^N$ of $\mathcal{S}$ as the time trajectories of the dynamical system evaluated at the locations x_i.

Given a discrete set $\mathcal{S}$ belonging to $\mathbb{R}^N$, the set $\{T_i\}_{i=1}^l$ is called a *clustering* or a *tessellation* of the set $\mathcal{S}$ if $T_i \subset \mathcal{S}$ for $i = 1, \cdots, l$, $T_i \cap T_j = \emptyset$ for $i \neq j$, and $\cup_{i=1}^l T_i = \mathcal{S}$. Let $|\cdot|$ denote the Euclidean norm on $\mathbb{R}^N$. Given a set of points $\{\mathbf{z}_i\}_{i=1}^l$ belonging to $\mathbb{R}^N$ (but not necessarily to $\mathcal{S}$), the *Voronoi region* V_i corresponding to the point $\mathbf{z}_i$ is defined by

$$V_i \quad = \quad \{\mathbf{y} \in \mathcal{S} \mid \quad |\,\mathbf{y} - \mathbf{z}_i\,| \quad \leq \quad |\,\mathbf{y} - \mathbf{z}_j\,| \qquad j = 1, \cdots, l, \quad j \neq i\},$$

where equality holds only for $i < j$. The points $\{\mathbf{z}_i\}_{i=1}^l$ are called *generating points* or *(cluster) generators.* Such a set $\{V_i\}_{i=1}^l$ is known as a *Voronoi tessellation* or *Voronoi clustering* of $\mathcal{S}$ and each V_i is referred to as the *Voronoi region* or *cluster* corresponding to $\mathbf{z}_i$.

Given a density function $\rho(y)$ defined on $\mathcal{S}$, for each cluster V_i, we can define its *cluster centroid* $\mathbf{z}_i^*$ by

$$\mathbf{z}_i^* = \frac{\sum_{\mathbf{y} \in V_i} \mathbf{y}\rho(\mathbf{y})}{\sum_{\mathbf{y} \in V_i} \rho(\mathbf{y})} \qquad i = 1, \cdots, l.$$

Given a set $\mathcal{S}$ of M vectors in $\mathbb{R}^N$ and a positive integer $l \leq M$, a *centroidal Voronoi tessellation* (CVT) or *centroidal Voronoi clustering* of $\mathcal{S}$ is a special Voronoi tessellation satisfying

$$\mathbf{z}_i = \mathbf{z}_i^* \qquad i = 1, \cdots, l \tag{2.1}$$

i.e., the generators of the Voronoi tessellation coincide with the centroids of the corresponding Voronoi clusters. It is important to note that general Voronoi tessellations do not satisfy the CVT property (2.1) so that, for given a set $\mathcal{S}$ and positive integer l, a CVT must be constructed. Algorithms for this purpose are discussed in subsection 2.2.

Centroidal Voronoi tessellations are closely related to minimizers of an "*energy*". Specifically, let

$$\mathcal{E}(\{\mathbf{z}_i\}_{i=1}^l, \{V_i\}_{i=1}^l) = \sum_{i=1}^{l} \sum_{\mathbf{y}\in V_i} |\mathbf{y} - \mathbf{z}_i|^2 \rho(\mathbf{y}), \tag{2.2}$$

where $\{V_i\}_{i=1}^l$ is a tessellation of $\mathcal{S}$ and $\{\mathbf{z}_i\}_{i=1}^l$ are points in $\mathbb{R}^N$. No a priori relation is assumed between the V_i's and the $\mathbf{z}_i$'s. We refer to $\mathcal{E}$ as the "*cluster energy*"; in the statistics literature, it is called the *variance* or *cost*. It is easy to prove that a necessary condition for $\mathcal{E}$ to be minimized is that $\{\mathbf{z}_i, V_i\}_{i=1}^l$ is a centroidal Voronoi tessellation of $\mathcal{S}$; see [13].

The connection between CVTs and reduced-order bases is now easily made. The set $\mathcal{S}$ is obviously the snapshot set. Then the CVT reduced basis set is the set of generators $\mathbf{z} = \{\mathbf{z}_i\}_{i=1}^l$ of a CVT of snapshot set $\mathcal{S}$. In the context of reduced basis modeling, the snapshots are solutions of the underlying dynamic systems (partial differential equations).

2.2. **Algorithms for constructing discrete CVTs.** As we have seen, the points that generate a Voronoi tessellation are not generally the centroids of the associated Voronoi regions. As a result, one is left with the following construction problem: given a region $\mathcal{S} \subset \mathbb{R}^N$ and a positive integer l, determine an $l-$point centroidal Voronoi tessellation of $\mathcal{S}$. Among many known methods for constructing centroidal Voronoi tessellations, we describe the two methods which are perhaps most "basic" and, certainly in the first case, the most used.

First, we have *Lloyd's method*[23] which is the straightforward iteration between constructing Voronoi tessellations and centroids.

Lloyd's method: Start with some initial set of l points $\{\mathbf{z}_i\}_{i=1}^l$ in $\mathcal{S}$, e.g., determined using random sampling;

(1) construct the Voronoi tessellation $\{V_i\}_{i=1}^l$ of $\mathcal{S}$ associated with the points $\{\mathbf{z}_i\}_{i=1}^l$;
(2) compute the centroids of the Voronoi regions $\{V_i\}_{i=1}^l$ found in Step 1; these centroids are the new set of points $\{\mathbf{z}_i\}_{i=1}^l$;
(3) go back to Step 1, or, if happy with convergence, quit.

Lloyd's method and its convergence properties have been analyzed; see [13] and [12] and also the references cited therein.

A second method is *McQuee's method* [24] which is a random sampling algorithm that doesn't require the explicit construction of Voronoi tessellations or of centroids.

McQueen's method: Start with some initial set of l points $\{\mathbf{z}_i\}_{i=1}^l$ in $\mathcal{S}$, e.g., determined using random sampling; set the integer array $J_i = 1 for i = 1, \cdots, l$;

(1) pick a random point $\mathbf{y} \in \mathcal{S}$;
(2) find the $\mathbf{z}_i$ closest to $\mathbf{y}$; denote the index of that $\mathbf{z}_i$ by i^*;
(3) set $\mathbf{z}_i \leftarrow \dfrac{J_{i^*} z_{i^*} + y}{J_{i^*} + 1}$ and $J_{i^*} \leftarrow J_{i^*} + 1$;
(4) $\mathbf{z}_{i^*}$ along with the unchanged points $\{\mathbf{z}_i\}_{i=1, i\neq i^*}^l$ are the new set of points;
(5) go back to Step 1, or, if happy with convergence, quit.

Note that J_i keeps track of how may times the point $\mathbf{z}_i$ has been previously updated. Remarkably (since neither Voronoi tessellations or centroids appear anywhere in the definition of the algorithm), the McQueen iterations converge to a set of generators of a CVT. The convergence properties of McQueen's methods have been analyzed in [24].

One point is sampled at each McQueen iteration so that the McQueen iterations are cheap, but lots of them are needed. Lloyd's method requires relatively fewer iterations, but each iteration is expensive; a straightforward implementation requires the explicit construction of Voronoi regions and, to determine the centroids, numerical integrations on polyhedra. Variations that utilize both features of the McQueen algorithm and the Lloyd algorithms have been given in [18].

So far, the density function was chosen by $\rho(\cdot) = 1$ (uniform density) in CVT reduced-order modelling. That is to say, cluster centroid is defined by

$$\mathbf{z}_i = \frac{1}{n_i} \sum_{\mathbf{y} \in V_i} \mathbf{y} \qquad \text{for} \quad i = 1, \cdots, l,$$

where V_i is Voronoi region, $\mathbf{y}$ is snapshot, and n_i denotes the cardinality of cluster V_i; clearly, $\sum_{i=1}^{l} n_i = M$, the cardinality of the set $\mathcal{S} = \{\mathbf{y}_i\}_{i=1}^{l}$. Also, the energy function is defined by (2.2) with $\rho(\mathbf{y}) = 1$.

For determining CVT's of discrete point sets that minimizes the energy function, we use the Lloyd's method.

Based on the earlier studies of CVT reduced-order modelling (see [21, 22], etc.), we can see that the l_2-norm errors (or l_2 relative errors) of the difference between the full finite element solution and the reduced-order solution exhibit strong oscillations during the simulation. For instance, errors at both ends (starting time and final time) can be quite different from those in between. Since the reduced-order basis vectors are not constructed with time evolution, we use the variable density (or nonuniform density) capability of CVT-based reduced-order modelling to obtain quasi-optimal reduced-order basis without much extra computing cost. In this paper, we choose a density (or weight) as follow

(1) Derive the reduced-order basis (centroids) by the Lloyd's algorithm with constant density ($\rho(\mathbf{y}_i) = 1$) from the set of snapshots $\mathcal{S} = \{\mathbf{y}_i^N(x) : i = 1, \ldots, M\}$;
(2) Compute the approximate solutions $\{\mathbf{y}^l\}$ using reduced-order basis (centroids);
(3) Compute the relative error at each time step,

$$E_i = \frac{||\mathbf{y}_i^N(x) - \mathbf{y}_i^l(x)||_{L^2(\Omega)}}{||\mathbf{y}_i^N(x)||_{L^2(\Omega)}}, \quad i = 1, \ldots, M \tag{2.3}$$

where $\mathbf{y}_i^N(x)$ and $\mathbf{y}_i^l(x)$ are the snapshots of full finite element solution and reduced order solution at each time step, respectively;
(4) Then, derive the density from the following formula:

$$\rho(\mathbf{y}_i) = \exp\left(E_i - \frac{1}{M} \sum_{i=1}^{M} E_i\right) \tag{2.4}$$

(5) Derive the reduced-order basis (centroids) by the Lloyd's algorithm with the density $\rho(\mathbf{y})$ from the set of snapshots $\mathcal{S}$;
(6) Compute the relative error (2.3). Go back to Step 4, or, stop if the stopping criterion is satisfied.

Here we want to find the density function which is uniformly distributed as much as possible. The $\mathbf{y}_i^l$ and $\mathbf{y}_i^N$ are CVT-ROM approximate solution and full order finite element approximate solution at spatial position x_i and time t respectively. Although the weight function (2.4) is not optimal for finding desired reduced-order basis, we use a feedback control idea to obtain a quasi-optimal reduced-order basis. For other approaches of adaptive density estimation, we refer to [15].

3. CVT-BASED MODEL REDUCTION FOR THE BURGERS EQUATION

3.1. **Generating snapshot sets.** We now turn our attention to the computations. We take the one dimensional Burgers equation as a model problem which has been used in other reduced modeling studies (see for example [5]). In order to generate a set of snapshots, we wish to numerically solve Burgers equation with nonhomogeneous Dirichlet boundary conditions on Ω. Consider Burgers equation

$$\frac{\partial y}{\partial t}(t,x) = \nu \frac{\partial^2 y}{\partial x^2}(t,x) - y(t,x)\frac{\partial y}{\partial x}(t,x) + f(t,x) \quad \text{for} \quad x \in \Omega, \quad t > 0, \tag{3.1}$$

$$y(t,0) = 0, \quad y(t,L) = u(t) \quad t > 0, \tag{3.2}$$

$$y(0,x) = y_0(x) \quad \text{for} \quad x \in \Omega. \tag{3.3}$$

where, Ω is the finite interval $[0, L]$.

Accurate Galerkin method finite element approximations of the solutions of (3.1)-(3.3) are obtained using the linear finite element ("hat" function) with N nodes. Finite element solutions are used for the generation of snapshots and later for comparison with CVT or POD based reduced-order solutions.

We assume the approximate solution of $y(t,x)$ is defined by

$$y^h(t,x) = u(t)\phi_{N+1}(x) + \sum_{i=1}^{N} c_i(t)\phi_i(x), \tag{3.4}$$

where $\phi_n(x)(n = 1, 2, \cdots, N+1)$ are the linear basis functions on the Ω, u is Dirichlet boundary condition, h is a discretization parameter and the coefficients $c_i(t)$ remain to be computed; for details, we refer to [4].

We use a variational formulation to define the finite element method to approximate (3.1). Integrating by parts and using homogeneous Dirichlet boundary conditions yield the weak

formulation of the problem,

$$\begin{aligned}\int_\Omega \frac{\partial y^h}{\partial t}(t,x)w(x)dx = &- \int_\Omega y(t,x)\frac{\partial y^h}{\partial x}(t,x)w(x)dx \\ &- \nu\int_\Omega \frac{\partial y^h}{\partial x}(t,x)\frac{\partial w}{\partial x}dx + \int_\Omega f(t,x)w(x)dx,\end{aligned} \tag{3.5}$$

where test function w are in a finite-dimensional subspace V_h of the Sobolev space $V = H_0^1(\Omega)$

Using (3.4), it is easy to see that (3.5) is equivalent to the system of nonlinear ordinary differential equations

$$\begin{aligned}&\sum_{i=1}^N \frac{d}{dt}c_i(t)(\phi_i,\phi_j) + \nu\sum_{i=1}^N c_i(t)(\frac{d\phi_i}{dx},\frac{d\phi_j}{dx}) \\ &+ (\sum_{i=1}^N c_i(t)\phi_i \sum_{k=1}^N c_k(t)\frac{d\phi_k}{dx},\phi_j) + u(t)\sum_{i=1}^N c_i(t)(\phi_{N+1}\frac{d\phi_i}{dx} + \phi_i\frac{d\phi_{N+1}}{dx},\phi_j) \\ &+ \frac{d}{dt}u(t)(\phi_{N+1},\phi_j) + \nu u(t)(\frac{d\phi_{N+1}}{dx},\frac{d\phi_j}{dx}) + u^2(t)(\phi_{N+1}\frac{d\phi_{N+1}}{dx},\phi_j) \\ &- (f,\phi_j) = 0, \qquad\qquad j = 1,\cdots,N,\end{aligned} \tag{3.6}$$

along with the initial conditions

$$\sum_{i=1}^N c_i(0)(\phi_i,\phi_j) = (y_0 - u(0)\phi_{N+1},\phi_j), \tag{3.7}$$

where $(\cdot,\cdot)$ denotes the $L^2(\Omega)$ inner product. The set of ordinary differential equations (3.6)-(3.7) is solved by using the Adams-Bashforth-Moulton method.

For the generation of snapshots, we will also solve, by the finite element method, stationary version of (3.1)-(3.3) for which the time derivative term in (3.1) and the initial condition (3.3) are omitted and u in (3.2) is chosen independent of t. The stationary version equation of (3.1)-(3.3) is solved easily by the Newton's method.

The M snapshot vectors

$$\mathbf{Z}_m = [c_1(t_m) \quad c_2(t_m) \quad \cdots \quad c_N(t_m) \quad u(t_m)]^T, \qquad m = 1,\cdots,M$$

are determined by evaluating the solution of equation (3.6)-(3.7) at M equally spaced time values $t_m, m = 1,...,M$, ranging from $t = 0$ to $t = T$. For subsequent use, it is convenient to modify the M snapshots so that they satisfy homogeneous boundary conditions. To this end, we first obtain the reference finite element approximation $v(x) = \sum_{i=1}^N v_k\phi_i(x)$ of the stationary equation of (3.1)-(3.2) with some constant boundary condition c. We then modify the M snapshots by

$$\mathbf{Z}_m \leftarrow (\mathbf{Z}_m - \frac{u(t)}{c}\mathbf{V}) \qquad for \quad m = 1,...,M.$$

where $\mathbf{V} = [v_1 \quad v_2 \quad \cdots \quad v_N \quad c]^T$

In this way, all the snapshots satisfy homogeneous boundary conditions.

3.2. **Determining reduced-order approximation.** We next apply the algorithms introduced in section (2.2) to determine a generators of the CVT from the given snapshot sets; a set of generators is to be used as a reduced order basis. Note that since the original boundary conditions have been "subtracted away," each basis function satisfies a zero Dirichlet boundary condition, In the interior of the region, each basis function satisfies the (discretized) continuity equation.

We assume that

$$y_{cvt}(t,x) = \beta(t)v(x) + \sum_{i=1}^{l} d_i(t)z_i(x),$$

where $v(x)$ is the steady-state solution of the Burger's equation, $\beta(t) = u(t)/c$, z_i denotes the $i-th$ CVT basis function, $d_i(t)$ is the corresponding coefficient, and l is the total number of CVT basis functions.

We consider the approximation Burger's equation

$$\begin{aligned}\int_\Omega \frac{\partial y_{cvt}}{\partial t}(t,x)z_j(x)dx = \; &- \int_\Omega y_{cvt}(t,x)\frac{\partial y_{cvt}}{\partial x}(t,x)z_j(x)dx \\ &+ \nu\int_\Omega \frac{\partial^2 y_{cvt}}{\partial x^2}(t,x)z_j(x)dx + \int_\Omega f(t,x)z_j(x)dx\end{aligned} \tag{3.8}$$

for $j = 1, \cdots, l$, where z_j are test function in subspace of V_h; for details see ([21]). Integrating by parts and using homogeneous Dirichlet boundary conditions yield the weak formulation of the problem,

$$\begin{aligned}&\sum_{i=1}^{N}\frac{d}{dt}d_i(t)(z_i,z_j) + \nu\sum_{i=1}^{N} d_i(t)(\frac{dz_i}{dx},\frac{dz_j}{dx}) \\ &+ (\sum_{i=1}^{N} d_i(t)z_i\sum_{k=1}^{N} d_k(t)\frac{dz_k}{dx}, z_j) + \beta(t)\sum_{i=1}^{N} d_i(t)(v\frac{dz_i}{dx} + z_i\frac{dv}{dx}, z_j) \\ &+ \frac{d}{dt}\beta(t)(v,z_j) + \nu\beta(t)(\frac{dv}{dx},\frac{dz_j}{dx}) + \beta^2(t)(v\frac{dv}{dx}, z_j) \\ &- (f,z_j) = 0, \qquad\qquad j = 1,\cdots,l,\end{aligned} \tag{3.9}$$

along with the initial conditions

$$\sum_{i=1}^{N} d_i(0)(z_i,z_j) = (y_0 - u(0)v, z_j), \tag{3.10}$$

where $(\cdot,\cdot)$ denotes the $L^2(\Omega)$ inner product.

Each basis, generator $\mathbf{Z}_i \in \mathbf{R}^N$ of a CVT, defined a finite element function, i.e., if $\mathbf{Z}_i = [Z_i^1 \quad Z_i^2 \quad \cdots \quad Z_i^N]^T, i = 1, \cdots, l$, we then have the corresponding finite element functions

$$z_i(x) \;=\; \sum_{j=1}^{N} Z_i^j \phi_j(x) \qquad \text{for } i \;=\; 1, \cdots, l.$$

and $v(x)$ is already made in section (3.1).

From the definition of the reduced-order basis, we theoretically could assure that the finite element approximation (3.5) agrees with the reduced-order approximation (3.8) (see [21]).

4. Computational Experiments

4.1. **Setting Up the Problem.** Consider the equation (3.1), we wish to compute approximate solutions of this problem to determine a set of snapshot vectors. The Galerkin finite element model was described in subsection 3.1 which results in a system of ordinary differential equations (3.9-3.10).

In our computational code, the numerical schemes are implemented in MATLAB and the ODEs (3.9)-(3.10) are solved using the Adams-Bashforth-Moulton method. The grid is chosen to be

$$x_i = \frac{i}{N+1} \quad \text{for} \quad i = 0, ..., N+1 \quad \text{and} \quad t_j = \frac{jT}{m} \quad \text{for} \quad j = 0, ..., m-1.$$

Most of the examples presented in this thesis employ numerical approximation schemes using $N = 79$ elements. This partitions the interval $[0, L]$ into 80 subintervals of uniform length. The result is $N = 79$ nodes, making (3.1) system of 79 ordinary differential equations. In this paper, the programs were written in MATLAB Version 7.1 executed on a INTEL(R) PENTIUM(R) 4 Series computer. As an example of the finite element solution, for the Burgers equation with the parameters $T = 1, \nu = 0.01, f = 0, u(t) = 0.3\sin(5t)$ and $y_0(x) = \sin \pi x$, the numerical solution to (3.9)-(3.10) is shown in Figure 1 in case of $N = 79, m = 80$.

4.2. **A Comparison to FEM Solutions.** The computation of CVT generators is discussed in the section 2.2. We derive the density from equation (2.4). Note that we take $\rho(\mathbf{y}) = 1$ in the CVT-uniform method.

In this subsection, we compare three reduced order methods (CVT-uniform, CVT-nonuniform and POD) of computation. The goal is to verify that different CVT schemes are converging to the FEM solution as the number of basis is increased. The CVT-uniform method, the CVT-nonuniform method and the POD method are compared for $l = 4, 8$ and 16 basis. We conclude that CVT-uniform, CVT-nonuniform and POD exhibit different accuracy for the three cases.

First of all, we apply the algorithms of subsection 2.3 to determine the generators of a CVT of the snapshot set which are then used as a reduced-order basis.

Table 1-6 compare, for the 4, 8, and 16 generator cases respectively, population and range of snapshot indices corresponding to each cluster. Note that the clusters are formed exactly from a sequence of data points at neighboring times.

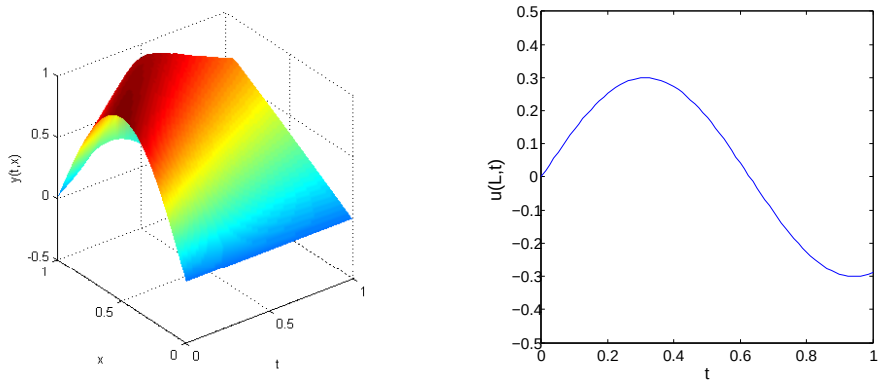

FIGURE 1. Full finite element solution of the Burgers equation (left), Boundary condition: $u(L,t) = 0.3sin(5t)$ (right).

TABLE 1. Cluster statistics for the 4 generators on CVT-uniform.

Cluster	Population	Range of snapshot indices
1	13	[1, 13]
2	13	[14, 26]
3	16	[27, 42]
4	38	[43,‧80]
total	80	[1, 80]

TABLE 2. Cluster statistics for the 4 generators on CVT-nonuniform.

Cluster	Population	Range of snapshot indices
1	14	[1, 14]
2	17	[15, 31]
3	37	[32, 68]
4	12	[69, 80]
total	80	[1, 80]

Now, two different CVTs having $l = 4, 8$ and 16 generators are determined. Figures 2, 3, 9 and 10 display, for the 4 and 8 generator cases respectively, the two types of CVT-basis computed from the snapshots. The solutions are not normalized. Figures 4 and 11 display, for the 4 and 8 generator cases, the POD basis computed from the same snapshot data.

It is important to note that, in contrast to the POD basis set, the CVT basis set of size 8 is not built by augmenting the CVT basis set of size 4; most of the elements of the larger set seem significantly different from any of those of the smaller set.

TABLE 3. Cluster statistics for the 8 generators on CVT-uniform.

Cluster	Population	Range of snapshot indices
1	7	[1, 7]
2	7	[8, 14]
3	6	[15, 20]
4	6	[21, 26]
5	8	[27, 34]
6	13	[35, 47]
7	21	[48, 68]
8	12	[69, 80]
total	80	[1, 80]

TABLE 4. Cluster statistics for the 8 generators on CVT-nonuniform.

Cluster	Population	Range of snapshot indices
1	6	[1, 6]
2	7	[7, 13]
3	8	[14, 21]
4	10	[22, 31]
5	11	[32, 42]
6	12	[43, 54]
7	16	[55, 70]
8	10	[71, 80]
total	80	[1, 80]

In some computations relating CVT and POD, we have a priori knowledge of the FEM solution. In this case, we measure the numerical error introduced by the two approximating schemes, calculating the relative l_2 error at time t given by formula (2.3) in section 2.2.

The errors are also shown graphically by computing $y^l(t,x)$ and $y^N(t,x)$ at $N+2$ evenly-spaced points in each subinterval. For the 4, 8, and 16 generator cases, the numerical solutions and the actual errors (the difference $y^l(t,x) - y^N(t,x)$) are plotted at these points for comparison. Figures 5, 6, 12 and 13 display, for the 4, and 8 generator cases respectively, the CVT-uniform and CVT-nonuniform solutions and the corresponding actual errors. Figures 7 and 14 display, for the 4 and 8 generator cases respectively, POD-based numerical solutions and the corresponding actual errors.

For the 4, 8, and 16 generator cases, the plots of l_2 errors versus time are displayed in Figures 8 and 15. Note that, l_2 errors decrease as the size of the reduced basis set is increased. Moreover, the very low-dimensional CVT-nonuniform-based reduced order solutions are seen to achieve considerable accuracy.

Table 7 compares the computational times for the CVT-uniform, CVT-nonuniform and POD methods using $l = 4, 8$ and 16. The speed for the CVT-uniform method at $l = 8$ is slightly

TABLE 5. Cluster statistics for the 16 generators on CVT-uniform.

Cluster	Population	Range of snapshot indices
1	2	[1, 2]
2	3	[3, 5]
3	3	[6, 8]
4	4	[9, 12]
5	4	[13, 16]
6	3	[17, 19]
7	3	[20, 22]
8	3	[23 , 25]
9	4	[26, 29]
10	4	[30, 33]
11	5	[34, 38]
12	7	[39, 45]
13	9	[46, 54]
14	11	[55, 65]
15	8	[66, 73]
16	7	[74, 80]
total	80	[1, 80]

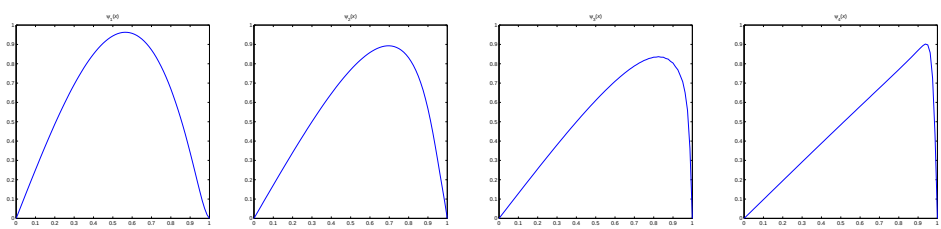

FIGURE 2. CVT-uniform basis functions for $l = 4$.

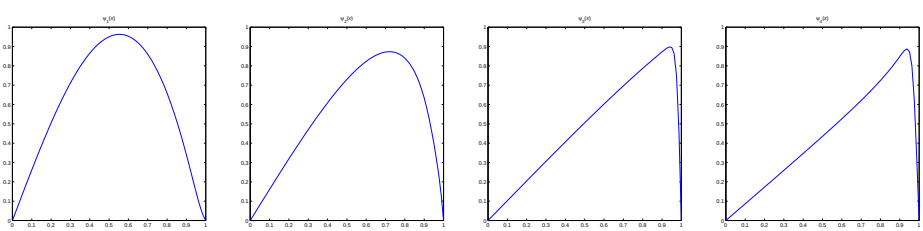

FIGURE 3. CVT-nonuniform basis functions for $l = 4$.

faster than other two methods CVT-nonuniform and POD. For the residue, the speeds are all similar for each cases.

TABLE 6. Cluster statistics for the 16 generators on CVT-nonuniform.

Cluster	Population	Range of snapshot indices
1	6	[1, 6]
2	6	[7, 12]
3	5	[13, 17]
4	5	[18, 22]
5	4	[23, 26]
6	5	[27, 31]
7	5	[32, 36]
8	4	[37 , 40]
9	5	[41, 45]
10	8	[46, 53]
11	7	[54, 60]
12	6	[61, 66]
13	4	[67, 70]
14	4	[71, 74]
15	3	[75, 77]
16	3	[78, 80]
total	80	[1, 80]

TABLE 7. Computation times.

the number of generator	method	computation time
$N = 80$	FEM	936.4218
$l = 4$	POD	0.4844
	CVT-uniform	0.6719
	CVT-nonuniform	0.5000
$l = 8$	POD	12.6875
	CVT-uniform	7.2031
	CVT-nonuniform	11.8125
$l = 16$	POD	69.7344
	CVT-uniform	67.7813
	CVT-nonuniform	75.1875

5. CONCLUSION

We have introduced and discussed a weighted (nonuniform density) centroidal Voronoi tessellation for low order approximate solution. We found that the approximate solution obtained by a weighted CVT-based reduced order model for Burgers equation is more accurate than that obtained by CVT uniform based reduced order model.

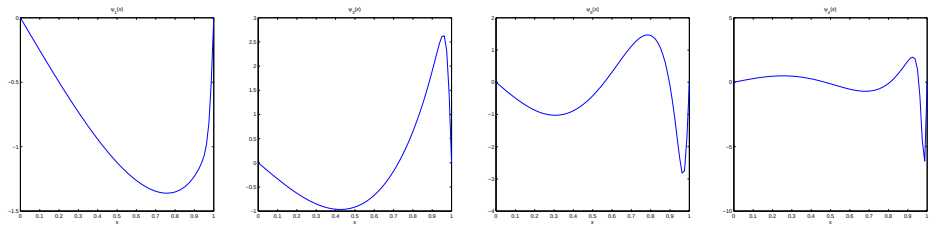

FIGURE 4. POD basis functions for $l = 4$.

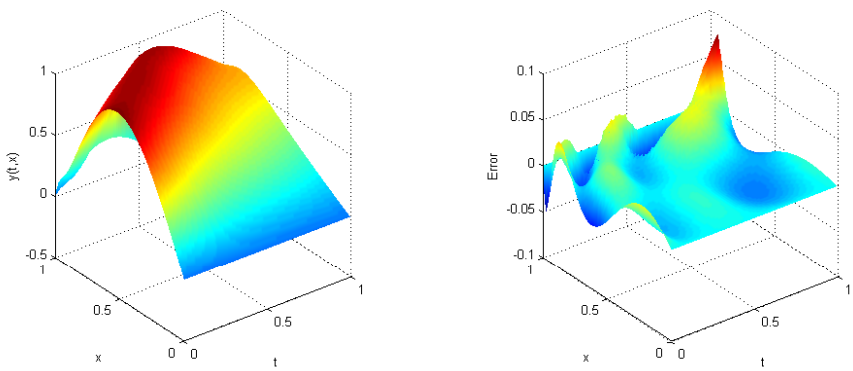

FIGURE 5. CVT-uniform-based reduced order solution (left) and actual errors using 4 generators.

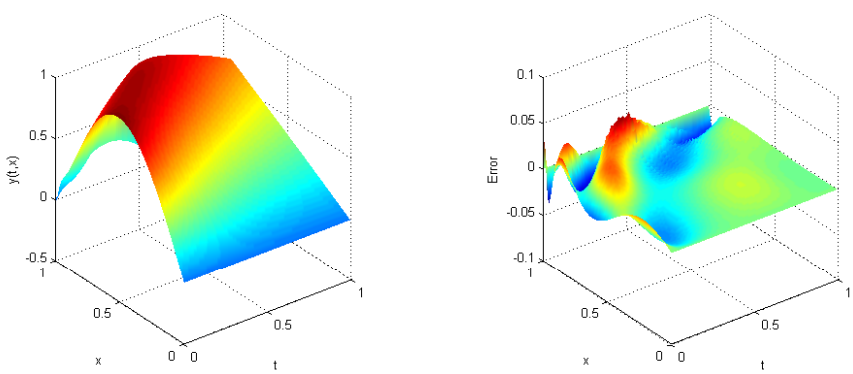

FIGURE 6. CVT-nonuniform-based reduced order solution (left) and actual errors using 4 generators.

Future efforts involve application of the reduced bases framework to more complex physical problems, such as those in fluid flows and materials processing, and more systematically interpreting how to choose the nonuniform density argument (nonconstant weight function).

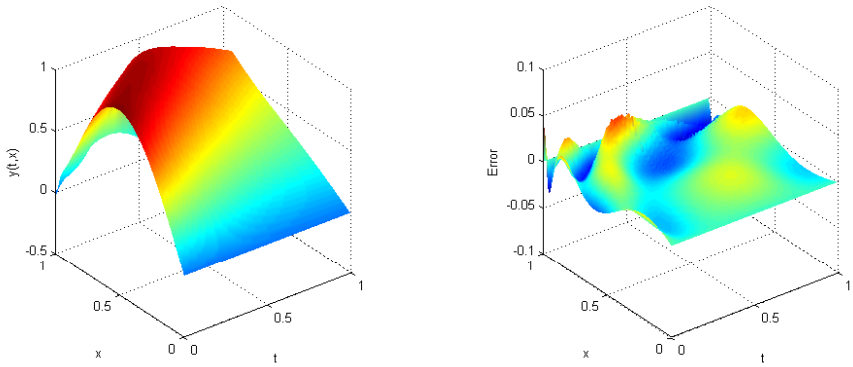

FIGURE 7. POD-based reduced order solution (left) and actual errors using 4 generators.

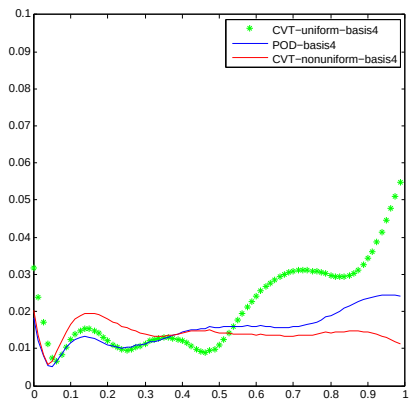

FIGURE 8. Relative errors for $l = 4$.

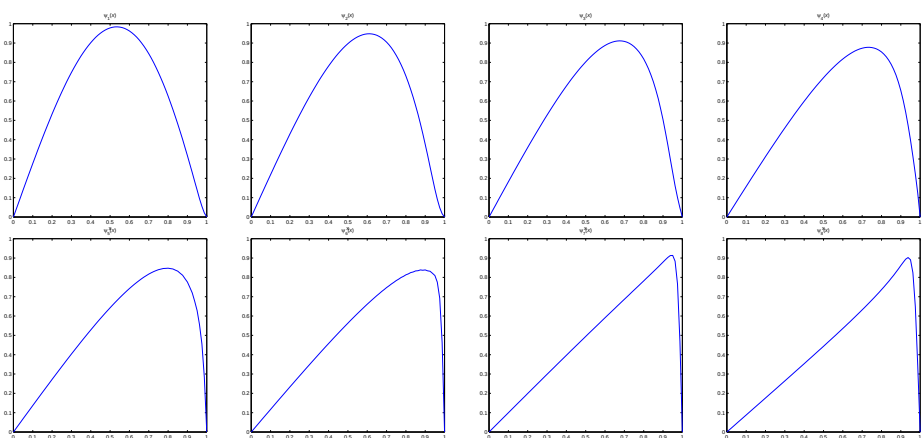

FIGURE 9. CVT-uniform basis functions for $l = 8$.

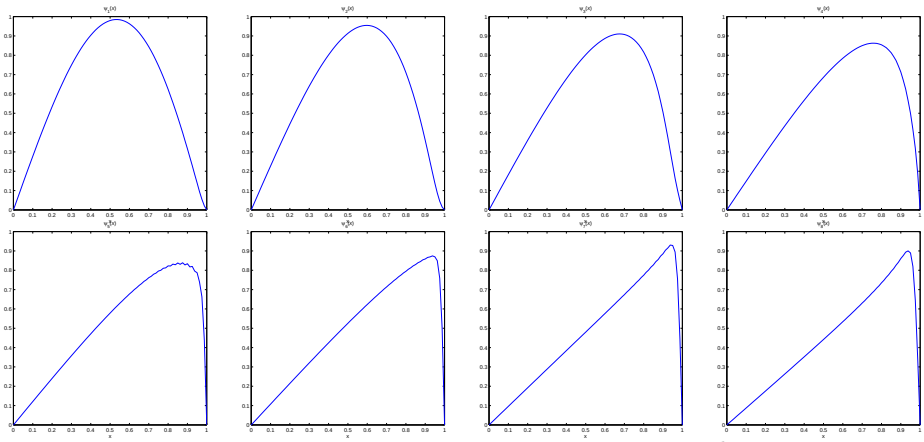

FIGURE 10. CVT-nonuniform basis functions for $l = 8$.

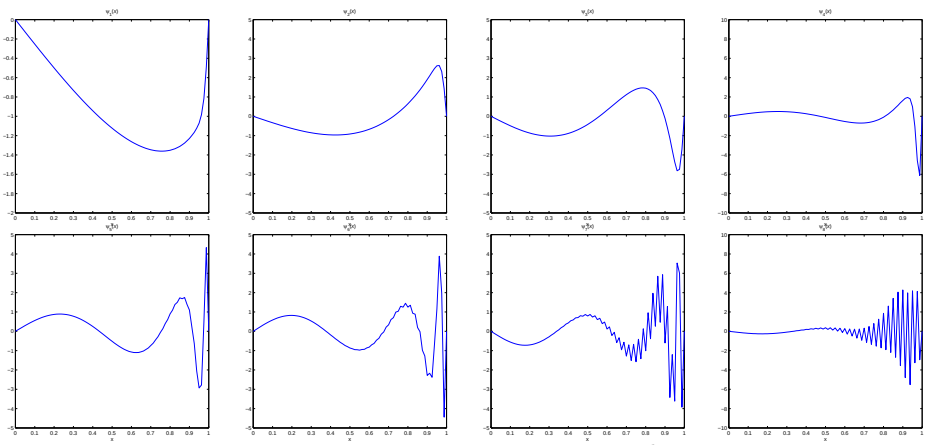

FIGURE 11. POD basis functions for $l = 8$.

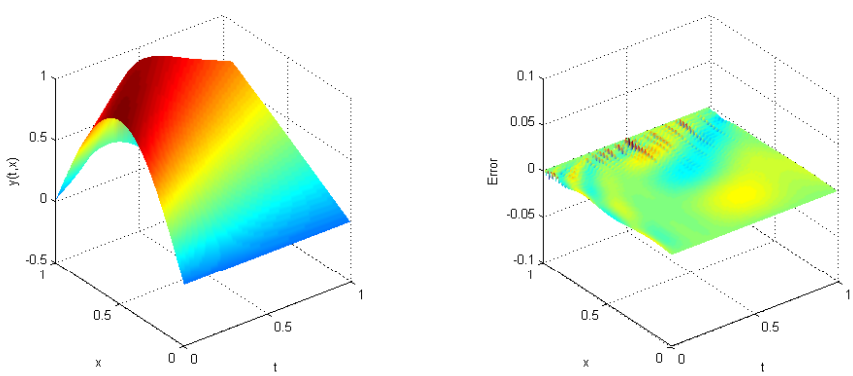

FIGURE 12. CVT-uniform based reduced order solution (left) and actual errors using 8 generators.

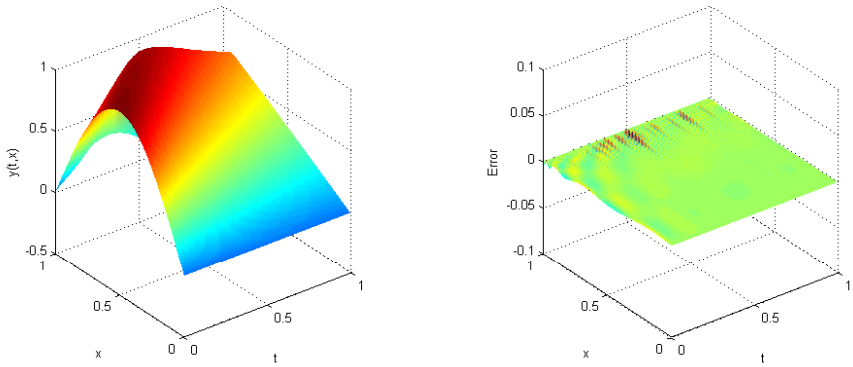

FIGURE 13. CVT-nonuniform based reduced order solution (left) and actual errors using 8 generators.

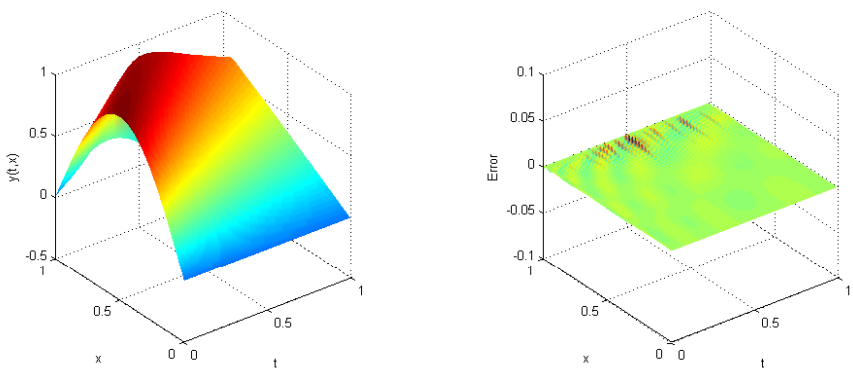

FIGURE 14. POD-based reduced order solution (left) and actual errors using 8 generators.

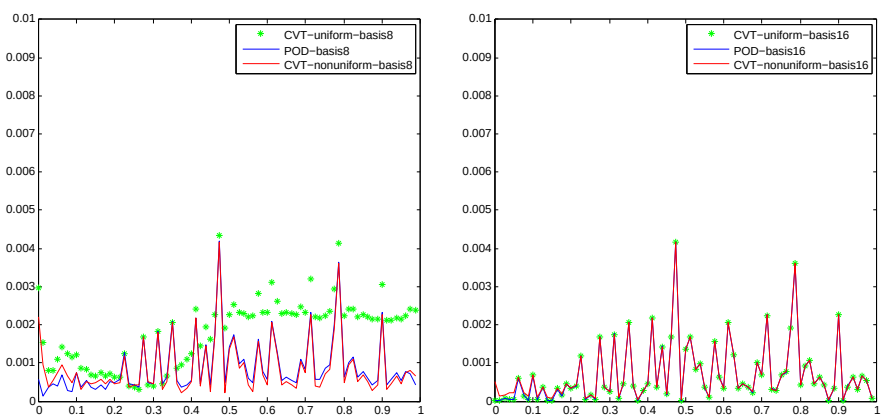

FIGURE 15. Relative errors for $l = 8$ (left) and $l = 16$ (right) .

Although the density (2.4) is not optimal in this article, we are obtained realatively accurate result for reduced-order modelling problems from the bases generated by weight. In any case, we will continue to research in future for finding the optimal weight function.

REFERENCES

[1] B. O. Almroth, Automatic choice of global shape functions in structural analysis, AIAA J., **16** (1979), 525-528.

[2] J. Atwell and B. King, Reduced order controllers for spatially distributed systems via proper orthogonal decomposition, SIAM J. Sci. Comput. **26** (2004), 128-151.

[3] A. K. Bangia, P. F. Batcho, I. G. Kevrekidis, and G. E. Karniadakis, Unsteady two-dimensional flows in complex geometries: comparative bifurcation studies with global eigen-function expansions, SIAM J. on Sci. Comput., **18** (1997), 775-805.

[4] S. C. Brenner and L. R. Scott, The mathematical theroy of finite element methods, Springer-Verlag, New York, 1994.

[5] J. Borggaard, A. Hay, and D. Pelletier. Interval-based reduced-order models for unsteady uid ow. International Jounal of Numerical Analysis and Modeling, **4** (2007), 353367.

[6] J. M. Burgers, Mathematical examples illustrating relations occuring in the theory of turbulent fluid motion, Trans. Roy. Neth. Acad. Sci. **17** (1939), Amsterdam, 1-53

[7] J. M. Burgers, A mathematical model illustrating the theory of turbulence, Adv. in Appl. Mech, **1** (1948), 171-199.

[8] J. M. Burgers, Statistical problems connected with asymptotic solution of one-dimensional nonlinear diffusion equation, in M. Rosenblatt and C. van Atta (eds.), Statistical Models and Turbulence, Springer, Berlin (1972), 41.

[9] J. Burkardt, Q. Du, M. Gunzburger and H.-C. Lee, Reduced Order Modeling of Complex Systems, in Proceeding of the 20th Biennial Conference on Numerical Analysis, Ed. by D F Griffiths & G A Watson, University of Dundee, June, 2003, 29-38.

[10] J. A. Burns and S. Kang, A control problem for Burgers equation with bounded input/oqtput, ICASE Report 90-45, 1990, NASA Langley research Center, Hampton, VA; Nonlinear Dynamics, **2** (1991), 235-262.

[11] C. T. Chen, Linear System Theory and Design, Holt, Rinehart and Winston, New York, NY, 1984.

[12] Q. Du, M. Emelianenko, and L. Ju, "Convergenece of the Lolyd algorithm for computing centroidal Voronoi tessellations, SIAM J. Numer. Anal., **44** (2006),. 102-119.

[13] Q. Du, V. Faber, and M. Gunzburger, Centroidal Voronoi Teesellations: applications and algorithms, SIAM Review **41** (1999), 637-676.

[14] Q. Du and M. Gunzburger, Model reduction by proper orthogonal decomposition coupled with centroidal Voronoi tessellation, Proc. Fluids Engineering Division Summer Meeting, FEDSM2002-31051, ASME, 2002

[15] Q. Du and X. Wang, Tessellation and Clustering by Mixture Models and Their Parallel Implementations, in Proceeding of the fourth SIAM international conference on Data Mining, L ake Buena Vista, FL, 2004, SIAM, 257-268.

[16] J. S. Gibson, The riccati integral equations for optimal control problems on Hilbert spces, SIAM Jounal on the Control and Optimazation, bf 17 (1979), 537-565.

[17] J. S. Gibson, and I. G. Rosen, Shifting the closed-loop spectrum in teh optimal linear quadratic regulator problem for hereditary system, Institute for Computer Applications for Science and Engineering, ICASE Report 86-16, 1986, NASA Langley Reserch Center, Hampton, VA.

[18] L. Ju, Q. Du and M. Gunzburger, Probabilistic methods for centroidal Voronoi tessellations and their parallel implementations, Parallel Computing, **28** (2002), 1477-1500.

[19] K. Kunisch and S. Volkwein, Control of burgers equation by a reduced order approach using proper orthogonal decomposition. J. Optim. Theory Appl. 102 (1999), 345–371.
[20] I. Lasiecka, and R. Triggiani, Dirichlet boundary control problem for parabolic equation with quadratic cost: analticity and Riccati's feedbacksynthesis, SIAMJ. Control and Optimization **21** (1983), 41-67.
[21] H.-C. Lee, J. Burkardt, and M. Gunzburger, Centroidal Voronoi tessellation-based reduce-order modeling of complex systems, SIAM J. Sci. Comput. **28** (2006), 459–484.
[22] H.-C. Lee, J. Burkardt, and M. Gunzburger, POD and CVT-based Reduced-order modeling of Navier-Stokes flows, Comput. Methods Appl. Mech. Engrg. **196** (2006), 337-355.
[23] S. Lloyd, Least squares quantization in PCM, IEEE Trans. Infor. Theory, **28** (1982), 129-137.
[24] J. MacQueen, Some methods for classification and analysis of multivariate observations, Proc. Fifth Berkeley Symposium on Mathematical Statistics and Probability, **1** (1967), University of California, 281-297.
[25] H. Marrekchi, Dynamic compensators for a nonlinear conservation law, Ph.D. Dissertation, Virginia Polytechnic Institute and State University, 1993.
[26] D. A. Nagy, Modal representation of geometrically nonlinear behavior by the finite element method, Computers and Structures, **10** (1979), 683-688.
[27] A. K. Noor, Recent advances in reduction methods for nonlinear problems, Computers and Structures, **13** (1981), 31-44.
[28] A. K. Noor, C. M. Andersen, and J. M. Peters, Reduced basis technique for collapse analysis of shells, AIAA J., **19**, 393-397.
[29] A. K. Noor and J. M. Peters, Reduced basis technique for nonlinear analysis of structures, AIAA J., **18**, 455-462.
[30] J. S. Peterson, The reduced-basis method for incompressible viscous flow calculations, SIAM J. Scientific and Statistical computing, **10** (1989), 777-786.
[31] R. Triggiani, and R. Bulrisch, Boundary feedback stabilizability parabolic equations, Appl. Math. Optim. **6** (1980), 201-220.